Crystallization Kinetics of PPS Composites and Quantification of Fiber Nucleation Density Using a Computer Simulation

NATHAN A. MEHL* and LUDWIG REBENFELD†

TRI/Princeton, and Department of Chemical Engineering, Princeton University, Princeton, New Jersey 08542

SYNOPSIS

Differential scanning calorimetry and hot-stage optical microscopy were used to study the isothermal crystallization kinetics of unreinforced poly(phenylene sulfide) (PPS) and PPS reinforced with aramid, carbon, and glass fibers. The influence that fibers have on the crystallization kinetics of PPS was found to depend on the characteristics of the fiber as well as the type of PPS used. For one kind of PPS, fibers enhanced the crystallization rate, while for another type of PPS, reinforcing fibers had a moderate depressing effect on the polymer crystallization rate. To clarify these effects, we used a new method of quantifying the nucleation process in fiber-reinforced composites that employs a 3-D computer simulation of spherulitic crystallization. Using this method, the nucleation density in the bulk polymer, N_b, and the nucleation density on fiber surfaces, N_f, were calculated for PPS composites as a function of crystallization temperature. The calculated values of N_b and N_f were used to explain differences in the effectiveness of the fibers as well as differences in the nucleating characteristics of the two polymers. © 1995 John Wiley & Sons, Inc.

INTRODUCTION

The ultimate properties of fiber-reinforced composite materials based on crystallizable thermoplastics are determined in part by the crystalline morphology of the polymer matrix,[1,2] which in turn depends on the rates of nucleation and crystal growth that define the crystallization kinetics. The nucleation and growth processes are governed by the thermal and mechanical processing conditions that are used but can also be influenced by the presence of reinforcing fibers. Due to their large surface-to-volume ratios and chemically active surfaces, reinforcing fibers have the potential to modify dramatically the crystallization characteristics of a given polymer matrix. Therefore, an understanding of the influence that fibers have on the crystallization kinetics of a polymer is an essential step in the optimization of composite material properties.

Recently, efforts have been made to characterize the effect of fiber reinforcement on the crystallization of a variety of thermoplastic polymers.[3-22] While experimental evidence confirms that fibers can influence the crystallization kinetics and morphology of the matrix polymer, conclusions about the effects of fibers from separate studies are often in disagreement. To understand better some of the discrepancies reported in the literature, an investigation of the influence that a variety of fibers have on the crystallization of two different types of poly(phenylene sulfide) PPS was undertaken. Previous studies of fiber-induced effects have used Ryton® PPS as the matrix polymer. The influence of fibers on the crystallization of Fortron® PPS is examined in this work. In addition, we wish to report a new technique, based on computer simulation, for quantifying fiber nucleation densities.

A review of the literature reveals that a number of groups have explored the effects of fibers on the crystallization kinetics of PPS. Jog and Nadkarni[3]

* To whom correspondence should be addressed.
† Present address: Milliken Chemical, 920 Milliken Road, Spartanburg, SC 29304.

Journal of Applied Polymer Science, Vol. 57, 187–199 (1995)
 CCC 0021-8995/95/020189-13

used differential scanning calorimetry (DSC) to measure the isothermal crystallization kinetics of a glass fiber/PPS matrix composite and unreinforced PPS. The glass-filled PPS system was found to crystallize 15–25% faster than unfilled polymer, as determined by the crystallization half-time. It was concluded that the acceleration in crystallization rate occurred because the glass fibers serve as nucleating agents for PPS. The effects of carbon fibers on the crystallization kinetics of PPS were investigated by both Kenny and Maffezzoli[4] and Caramaro et al.[5] In their study, Kenny and Maffezzoli[4] found that the presence of carbon fibers slowed the isothermal crystallization of PPS. In addition, the Avrami exponent of PPS in carbon fiber composites was lower than the Avrami exponent of the unreinforced polymer. When Caramaro et al.[5] analyzed the nonisothermal crystallization kinetics of carbon fiber-reinforced PPS, they found that the Avrami exponent of PPS was generally lower in the reinforced system than in unreinforced PPS. Desio and Rebenfeld[6-8] conducted a thorough investigation of PPS crystallization kinetics in composites based on sized and unsized aramid, carbon, and glass fibers. Their results indicate that the effects of fibers on the isothermal crystallization kinetics of PPS depend on both the fiber type and the surface treatment. In general, the crystallization rate of PPS in the fiber-reinforced systems was faster than unreinforced PPS. In addition, the presence of sizing on the fibers further increased the rate of crystallization. Finally, the Avrami exponent of PPS in all the reinforced systems was lower than the Avrami exponent of unreinforced PPS. Most recently, Auer et al.[9] used DSC to measure the crystallization kinetics of PPS in glass, carbon, and aramid-reinforced composites. In agreement with Desio and Rebenfeld,[6-8] they found that aramid fibers dramatically enhanced the crystallization rate of PPS. This result was attributed to a high nucleation density along the surface of the aramid fibers.

EXPERIMENTAL

Materials

Two types of PPS were used in this study, a grade of Ryton® supplied by Phillips Petroleum and Fortron® W214 supplied by Hoechst Celanese. The Fortron® resin differs from the classic Ryton® in its lower degree of branching,[23] although Phillips now also offers a more linear grade of Ryton®. Neat Ryton® PPS resin was supplied in 50-μm-thick film, and Fortron® PPS was compression molded from granular pellets into 75-μm-thick film. The reinforcing fibers were "PPS compatible"-sized glass fibers from Owens-Corning Fiberglas Corp.; sized AS-4 high-strength carbon fibers supplied by Hercules, Inc.; spin-finish-sized Kevlar® 49 aramid fibers from DuPont; and graphitized Thornel® T300 carbon fibers furnished by Amoco Performance Products. Scanning electron photomicrographs indicate that the macroscopic surface structure of the first three fiber types is smooth and featureless, while the surface of the Thornel® fibers has a rough, corrugated appearance.

Model Composite Preparation

The model PPS composites used to make DSC specimens were prepared using a compression molding procedure.[24] The molding procedure used to prepare model composites with unidirectional fiber orientation was as follows. Several fiber tows were evenly distributed (with uniaxial orientation) between two pieces of PPS film and placed in an aluminum mold. All surfaces of the mold in contact with the polymer were sprayed with a commercially available mold release agent, Frekote FRP. The mold was held at 310°C and 60 lb_f for 3 min using a PHI hot press and then cooled to room temperature. The model composite systems that were prepared using this procedure are shown in Table I. Unfortunately, only a limited supply of Thornel® fiber was available, so Thornel® reinforced Fortron® composites could not be produced. To insure identical thermal histories and to allow valid comparisons, unreinforced PPS samples were subjected to the same molding procedure as the reinforced systems.

Isothermal DSC Analysis

Neat and composite PPS specimens weighing 15 ± 0.3 mg were enclosed in aluminum DSC pans. The

Table I Model Composite Systems

Composite System	Wt Fraction Fibers	Vol Fraction Fibers	Fiber Diameter (μm)
Ryton®/Thornel®	0.58	0.51	8.0
Ryton®/Kevlar®	0.54	0.53	12.0
Ryton®/AS-4	0.52	0.45	8.0
Ryton®/Glass	0.60	0.45	15.0
Fortron®/Kevlar®	0.54	0.53	12.0
Fortron®/AS-4	0.60	0.53	8.0
Fortron®/Glass	0.67	0.52	15.0

specimens were heated to a melting temperature of 330°C for 2 min and then cooled at 320°C/min to the isothermal crystallization temperature of interest. Additional aluminum pan lids with a total weight of approximately 15 mg were placed in the reference pan as a means of improving the thermal response to the rapid quench. Because PPS crystallization rates are known to be affected by thermal treatment,[25] data were gathered only from the first crystallization run. The environment in the DSC cell during crystallization was, in all cases, high-purity dried nitrogen. By careful control of important variables such as sample weight, reference weight, and thermal treatment, it was possible to measure crystallization half-times of the DSC samples with high reproducibility, reflected by an average coefficient of variation of ±8%.

The crystallization rate of PPS is strongly affected by temperature, and therefore a temperature window exists in which isothermal kinetic data can be measured using the DSC. The upper temperature limit occurs because the DSC can detect only a finite rate of heat flow from the sample, and the lower temperature limit exists because the DSC cannot stabilize thermal conditions before crystallization begins. Differences in the crystallization rates of Ryton® and Fortron® cause differences in their crystallization windows, which are (215°C to 240°C) and (250°C to 265°C), respectively.

Spherulitic Growth Rate Measurement

The configuration of experimental equipment used to measure spherulitic growth rates was designed to approximate closely the conditions experienced by samples crystallizing in the DSC.[24] Thin films of PPS were placed between a glass slide and coverslip and then melted in an oven. Samples were melted at either 330 ± 2°C or 345 ± 2°C while exerting a slight pressure on the coverslip to reduce the film thickness. After 2 min in the melt, the slides were rapidly transferred to a nearby Mettler FP2 hot stage held at the desired isothermal crystallization temperature. Spherulitic growth was observed using a Zeiss Axioscope optical microscope equipped with long working distance objective lenses and recorded on videotape. The sizes of the growing spherulites were measured using a Video Micrometer from Colorado Video Inc. For each specimen, the growth rates of three to seven spherulites were determined by plotting their diameters as a function of time and then calculating the slope of the best-fit straight line. Sample-to-sample reproducibility of the growth rate measurements indicates a standard deviation of less than 6%. The hot-stage temperature controller was calibrated using an indium standard and a thermocouple. Since PPS is known to degrade when subjected to multiple heatings at elevated temperatures,[25] individual samples were used for only one growth rate experiment. To estimate the effective cooling rate that the samples experienced, a thermocouple was used to monitor the temperature of a glass slide during the quench. The change in temperature during rapid transfer to the hot stage was found to be insignificant. It was also determined that the rapid transfer technique allowed the microscope slide to reach a temperature 0.5°C above the desired isothermal temperature in 15 s after transfer to the hot stage, giving an average cooling rate of 300°C/min, which is about the same as that used with the DSC.

EXPERIMENTAL RESULTS

Effect of Fibers on Crystallization Kinetics of PPS

Differential scanning calorimetry was used to quantify the influence of fibers on the crystallization kinetics of Ryton® and Fortron® PPS. While a similar investigation of the crystallization rates of fiber-reinforced Ryton® has been reported,[7,8] portions of the study were repeated to compare the crystallization kinetics of Ryton® and Fortron® in composites that had experienced the same thermal history.

Ryton® PPS Crystallization

In general, the crystallization kinetics of Ryton® PPS were found to be significantly enhanced by the presence of reinforcing fibers. As demonstrated in Figure 1, the PPS crystallized in all of the composite

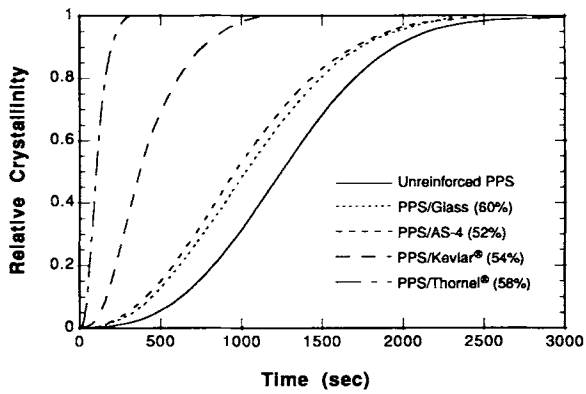

Figure 1 Effect of fibers on the crystallization rate of Ryton® PPS at 240°C. The fiber content is expressed in wt %.

systems reaches a given relative crystallinity faster than the corresponding unreinforced polymer. At a crystallization temperature of 240°C, the presence of Thornel® and Kevlar® fibers dramatically enhances the rate of crystallization of the base polymer. AS-4 carbon and glass fibers also increase the crystallization rate of PPS, but to a lesser extent. Evidently, the physical and chemical nature of the fiber surface must in some way influence the polymer crystallization process.

Reinforcing fibers were also found to have a strong influence on crystallization kinetics at other temperatures. The crystallization half-time, inversely related to the rate of crystallization, was used as a basis for comparing crystallization kinetics in reinforced and unreinforced Ryton® as a function of temperature. A plot of $t_{1/2}$ as a function of isothermal crystallization temperature that summarizes the kinetic data for Ryton® systems is shown in Figure 2. The crystallization half-time increases as a function of temperature for unreinforced PPS as well as for all the reinforced systems studied. This temperature dependence is expected because the driving force for polymer crystallization in this range of crystallization temperatures is a function of the undercooling from the equilibrium melt temperature ($T_m^\circ - T_c$).[26] Over the whole range of isothermal crystallization temperatures studied, Ryton® PPS reinforced systems crystallize faster than corresponding unreinforced Ryton®. The presence of the various fibers enhances the rate of crystallization of the base polymer, and the enhancement becomes more pronounced with increasing temperature. These observations of the relative degrees of rate enhancement from various types of reinforcing fibers are in qualitative agreement with similar data presented earlier.[7] In the current study, AS-4 fibers were found to be less effective at increasing the rate of crystallization than Desio and Rebenfeld reported, but the disagreement is likely a consequence of the different thermal processing conditions used. The time and temperature a polymer spends in the melt are known to influence the crystallization kinetics of the base polymer,[25] and they are also likely to affect the fiber-induced nucleation process.

The crystallization kinetics of reinforced and unreinforced Ryton® were examined in greater detail using the Avrami equation,

$$1 - C = \exp(-Kt^n) \qquad (1)$$

where C is the relative crystallinity, t is the time since the onset of nucleation, and n and K are constants diagnostic of the crystallization mechanism.

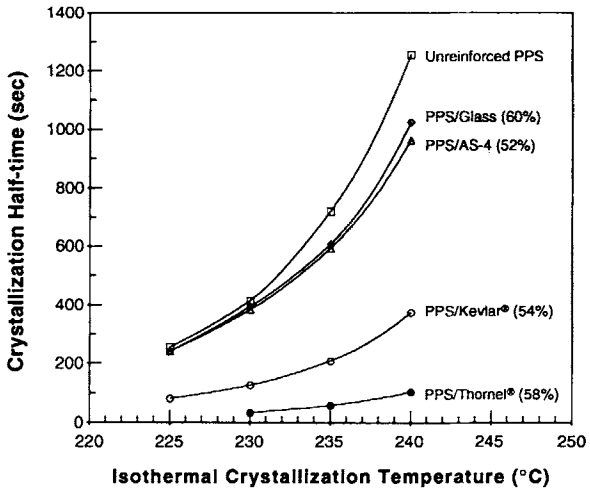

Figure 2 Crystallization half-time as a function of isothermal crystallization temperature for unreinforced Ryton® PPS and Ryton® composites. The fiber content is expressed in wt %.

The Avrami exponent, n, depends on the mechanism of nucleation and on the geometry of crystal growth; and the Avrami rate constant, K, contains nucleation and growth parameters. If the crystallization kinetics of a semicrystalline polymer follow the Avrami model, a plot of $\ln(-\ln(1-C))$ as a function of $\ln t$ should be linear with slope n. When Ryton® crystallization data were represented in this manner, the plots were similar to those of Desio and Rebenfeld;[6,8] Avrami plots of unreinforced PPS and PPS reinforced with either glass or AS-4 fibers are linear, while the Avrami plots of the PPS reinforced with either Kevlar® or Thornel® fibers are nonlinear.[24] Thus, fibers that have a strong enhancing effect on the crystallization rate of Ryton® PPS exhibit a nonlinear Avrami plot, while fibers that have a weak enhancing effect on the crystallization rate exhibit a linear Avrami plot.

Reinforcing fibers were also found to modify the Avrami parameters of Ryton® PPS. Table II presents the Avrami exponent for unreinforced and reinforced Ryton® as a function of crystallization temperature. The average error in calculating n was approximately ±5%. For all crystallization temperatures and in all systems studied, the Avrami exponent of the fiber-reinforced systems was lower than that of the unreinforced system by a statistically significant amount. This observation is consistent with previous experimental work[4–6,8] and with the predicted Avrami exponent of spherulites crystallizing in a constrained environment.[27,28] Stein and Powers[27] and Billon et al.[28] have shown that the Avrami exponent of athermally nucleated

Table II Summary of Avrami Exponents for Ryton® and Fiber-Reinforced Ryton® Composites

System	225°C	230°C	235°C	240°C
Ryton® PPS	2.9	2.8	2.8	2.7
Ryton®/Thornel® (58%)	—	2.3	2.3	2.5
Ryton®/Kevlar® (54%)	2.3	2.3	2.3	2.4
Ryton®/AS-4 (52%)	2.4	2.5	2.3	2.2
Ryton®/Glass (60%)	2.6	2.4	2.5	2.3

The Avrami exponent was calculated for $0.03 < C < 0.60$.

Table III Summary of Avrami Rate Constants for Ryton® and Fiber-Reinforced Ryton® Composites

System	225°C	230°C	235°C	240°C
Ryton® PPS	120	26	6.6	1.8
Ryton®/Thornel® (58%)	—	26000	7700	1800
Ryton®/Kevlar® (54%)	4200	1500	410	88
Ryton®/AS-4 (52%)	280	68	37	15
Ryton®/Glass (60%)	130	53	22	10

The Avrami rate constant was calculated for $0.03 < C < 0.60$. All values have been multiplied by 10^4. Units of K are min^{-n}.

spherulites that have been constrained to grow in thin films varies from 3 to 2 as the film thickness decreases. In addition, computer simulations of athermally nucleated spherulites in fiber-reinforced systems have demonstrated that fibers cause a decrease in the Avrami exponent.[24,29,30] Later, it will be shown that the mode of nucleation in the experimental PPS composites is, to a good approximation, athermal.

While the Avrami exponent is lower in fiber-reinforced Ryton® than in the unreinforced polymer, the Avrami rate constant is significantly higher in fiber-reinforced systems. Table III shows how the Avrami rate constant for unreinforced and reinforced Ryton® varies as a function of crystallization temperature. The average error in calculating K was approximately ±10%. Care must be taken when comparing Avrami rate constants because the units of the rate constant include the value of the Avrami exponent. However, small differences in n do not significantly influence the trends observed within and between systems. For all systems, the Avrami rate constant decreases with increasing crystallization temperature. In addition, at a given crystallization temperature, the rate constant is higher in the fiber-reinforced systems than in the unreinforced polymer. These observations are consistent with the crystallization half-time data since the Avrami rate constant can be viewed as a measure of the crystallization rate.

Fortron® PPS Crystallization

Unlike the crystallization kinetics of Ryton®, crystallization rates of Fortron® PPS are not strongly influenced by the presence of fibers. Figure 3 shows a comparison of the crystallization rates of reinforced and unreinforced Fortron® at a crystallization temperature of 260°C. In contrast to Figure 1, which presents a similar plot for Ryton® systems, the reinforced Fortron® systems crystallize at a slower rate than the unreinforced polymer. It is noteworthy that the same fibers that have such a dramatic positive effect on the crystallization rate of Ryton® have a modest negative effect on the crystallization rate of Fortron®.

Reinforcing fibers also have a negligible influence on the bulk rate of crystallization at other temperatures. A plot of $t_{1/2}$ as a function of crystallization temperature for unreinforced Fortron® and Fortron® composites is shown in Figure 4. For the entire range of crystallization temperatures studied, the reinforced systems crystallized more slowly than the neat polymer. As will be shown later, it is likely that the high nucleation density of Fortron® overwhelms the additional nucleation sites provided by the fiber surface. Although the crystallization half-times of

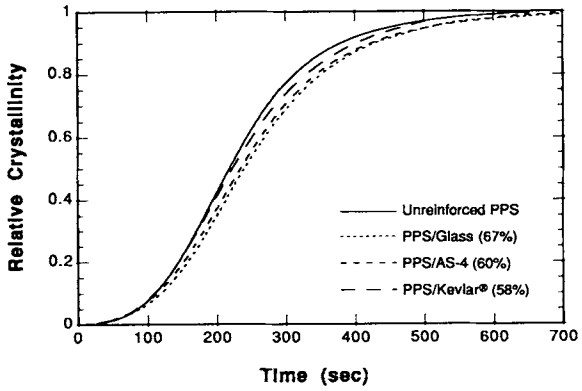

Figure 3 Effect of fibers on the crystallization rate of Fortron® PPS at 260°C. The fiber content is expressed in wt %.

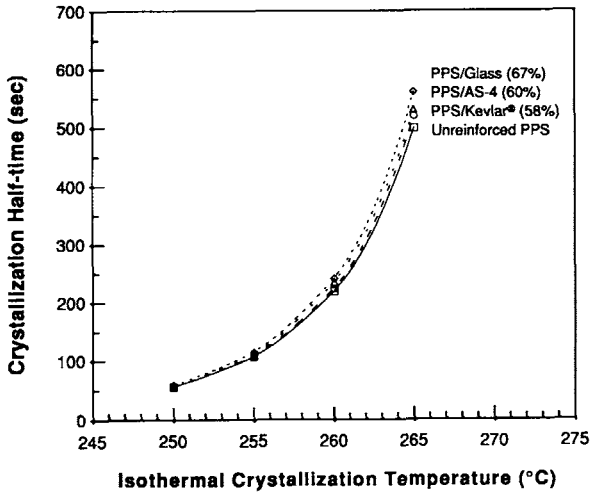

Figure 4 Crystallization half-time as a function of isothermal crystallization temperature for unreinforced Fortron® PPS and Fortron® composites. The fiber content is expressed in wt %.

the composite systems were higher than those of the unreinforced polymer, the relative ranking of crystallization rates in the Fortron® reinforced systems is the same as that observed for Ryton® composites. Kevlar® fiber-reinforced systems are faster crystallizers than AS-4 reinforced systems, which are faster crystallizers than glass-reinforced systems. Therefore, it appears that the various reinforcing fibers do have a minor influence on the crystallization rate of Fortron® composites, but the effect is of a much smaller relative magnitude than that observed in Ryton® crystallizations.

When the crystallization kinetics of Fortron® systems were analyzed with the Avrami model, Avrami plots for the unreinforced and reinforced polymer were essentially indistinguishable.[24] The slopes of the Avrami plots were found to be constant up to a relative crystallinity of about 0.6 and then began to decrease gradually as secondary crystallization became important. The Avrami exponents and rate constants for Fortron® systems as a function of isothermal crystallization temperature are shown in Tables IV and V. At all crystallization temperatures, except perhaps 265°C, the Avrami parameters of the reinforced systems are virtually the same as those of the neat polymer. This is consistent with the conclusion from the crystallization half-time data that the nucleation density of Fortron® PPS is high enough to nearly eliminate the influence of fibers. Also, theoretical derivations and computer simulations predict a negligible change in the Avrami exponent for high-nucleation-density spherulites growing in a constrained environment.[24,28-30]

Table IV Summary of Avrami Exponents for Fortron® and Fiber-Reinforced Fortron® Composites

System	250°C	255°C	260°C	265°C
Fortron® PPS	2.8	2.8	2.8	2.7
Fortron®/Kevlar® (58%)	2.7	2.8	2.7	2.3
Fortron®/AS-4 (60%)	2.8	2.7	2.6	2.2
Fortron®/Glass (67%)	2.7	2.6	2.6	2.5

The Avrami exponent was calculated for $0.03 < C < 0.60$.

COMPUTER SIMULATION MODELING

The experimental studies demonstrate that the influence of reinforcing fibers on the crystallization kinetics of PPS depends on the type of PPS used. For Ryton® PPS composites, fibers can dramatically enhance the polymer crystallization rate; however, for Fortron® composites, reinforcing fibers have a moderate depressing effect. This qualitative difference in fiber effects is likely a result of differences in the nucleation characteristics of the two polymers. As demonstrated by means of computer simulations,[24,29-32] it is primarily the relationship between the nucleation density on the fiber surface, N_f, and the nucleation density in the bulk polymer, N_b (or the rates of nucleation in the bulk and on fiber surfaces in the case of thermal nucleation), that determines whether fibers enhance or depress the crystallization rate of a reinforced polymer relative to that of an unreinforced polymer. To clarify these effects, we propose a new method of quantifying the nucleation process that occurs in fiber-reinforced PPS composites. The method is based on a com-

Table V Summary of Avrami Rate Constants for Fortron® and Fiber-Reinforced Fortron® Composites

System	250°C	255°C	260°C	265°C
Fortron® PPS	8500	1300	190	25
Fortron®/Kevlar® (58%)	7400	1300	210	48
Fortron®/AS-4 (60%)	7700	1100	210	66
Fortron®/Glass (67%)	7300	1100	180	50

The Avrami rate constant was calculated for $0.03 < C < 0.60$. All values have been multiplied by 10^4. Units of K are min^{-n}.

parison between experimental crystallization kinetic data and crystallization kinetic data predicted with the computer simulation. For the purposes of this study, we assume that the mode of nucleation in the bulk and on fiber surfaces is athermal and that the spherulitic growth rate is constant. It will be demonstrated that these assumptions are valid in the range of crystallization temperatures and for the PPS systems used in this study.

The Approach

Using several well-accepted assumptions about spherulitic crystallization, the primary crystallization kinetics of an athermally nucleated fiber-reinforced polymer can be completely characterized with five parameters.[29,30] These parameters are G, the radial spherulitic growth rate; N_b, the nucleation density per unit volume in the polymer bulk; N_f, the nucleation density per unit fiber surface area; V_f, the volume fraction of fibers; and D, the fiber diameter. To use our computer simulation to model experimental crystallization kinetic data, the five parameters must be determined for the experimental system. The volume fraction of fibers and the fiber diameter can be specified, and there exist several well-established methods for measuring or estimating the spherulitic growth rate and bulk nucleation density of a polymer. The fiber nucleation density, however, is generally difficult if not impossible to quantify rigorously. This is unfortunate because the fiber nucleation density can obviously have a great impact on the crystallization of a reinforced polymer and can therefore have an important influence on composite properties.

Fiber nucleation densities can be approximated using a crude method in which an optical microscope is used to count the number of visible fiber-nucleated spherulites that appear in a thin film composite sample and then normalizing this number by the surface area of the fiber. The method is unreliable for several reasons. First, the process of physically counting densely nucleated spherulites is hindered by the theoretical maximum resolving power of the optical microscope. In addition, because the observed image is a 2-D projection of a 3-D system, spherulitic growth in one area of the specimen may be obscured by the fiber or by the growth of other spherulites. Finally, large variations in fiber nucleation density are observed in the relatively small optical fields so that data from many independent experiments must be averaged to arrive at a reliable value. Despite these problems, it is possible to estimate fiber nucleation densities using the counting method. For example, Avella et al.[33] used such an approach to quantify the number of bulk and fiber nuclei that appeared in composites based on single Kevlar® fibers embedded in thin samples of polypropylene film. Nevertheless, one must question whether a fiber nucleation density measured from thin films is valid in fiber-reinforced polymers of a more realistic geometry.

We propose a different approach of estimating the fiber nucleation density in which a three-dimensional computer simulation of spherulitic crystallization[24,30] is used to model experimental crystallization data. The idea is to first measure four (G, N_b, V_f, and D) of the five controlling parameters for the fiber-reinforced PPS composites. Next, computer simulations are conducted for reinforced systems in which four of the controlling parameters are set to the values measured experimentally and the fifth parameter, the fiber nucleation density, is allowed to vary. Experimental crystallization kinetic data are then compared to the sets of data predicted with the computer simulation, and the fiber nucleation density corresponds to the simulated data which best agrees with the experimental crystallization data.

Measurement of four of the five controlling parameters in the experimental composite systems was conducted as follows. Fiber diameters were determined using electron microscopy. The fiber volume fractions, calculated from the fiber weight fractions, are known. Table I presents values of D and V_f for all the composite systems that were studied. Hot-stage optical microscopy was used to measure spherulitic growth rates. Finally, the bulk nucleation densities were estimated from an equation that relates the Avrami rate constant and the spherulitic growth rate. More complete descriptions of the techniques used to estimate the bulk and fiber nucleation densities are presented in the sections that follow.

Growth Rates of Ryton® and Fortron® PPS

Growth rate measurements of Ryton® spherulites were straightforward, due in part to the relatively low nucleation density of the polymer. At all temperatures investigated, growth rates were constant with time. Ryton® growth rates were also found not to be strongly affected by melting temperature. Increasing the melting temperature from the standard 330°C to 345°C significantly reduced the nucleation density but had no detectable effect on the spherulitic growth rate at a given crystallization temperature.

Unlike for the case of Ryton®, it was difficult to observe growing Fortron® spherulites with the hot-stage microscope, even for extremely thin films. Under rare circumstances, it was possible to find a small area of polymer in which the nucleation density was low enough to allow spherulites to grow large enough for observation, but this required many trials. It has been suggested that holding a polymer at a higher melt temperature before isothermal crystallization is useful in lowering the polymer nucleation density and hence allowing spherulites to grow to larger sizes.[11,34] We also observed that the number of spherulites in the field of view decreased with increasing melt hold temperature. By heating the Fortron® PPS to 345°C, we could more easily find regions of sufficiently low nucleation density to measure successfully the spherulitic growth rate. The values of G that we measured after heating the polymer to 345°C were in good agreement with the limited number of growth rate measurements that we were able to make after heating the polymer to 330°C. Thus, like Ryton®, Fortron® growth rates were found not to depend on melt temperature. However, the growth rate was lower in recycled samples that had previously experienced high melt temperatures, presumably due to polymer degradation and/or crosslinking.

Spherulitic growth rates of Ryton® and Fortron® as a function of crystallization temperature are summarized in Figure 5. As theory suggests, the spherulitic growth rates decrease as the temperature approaches the equilibrium melting point.[26] The dependence of growth rate on temperature is in qualitative agreement with previous data for PPS,[35,36] and the reported values are of the same magnitude. The growth rates measured in this study do not agree absolutely with the previous data, but the discrepancies are likely to be the result of the differences in the molecular weight distributions. Molecular weight has been shown to cause large effects on the spherulitic growth rates of PPS.[35,36]

Mode of Nucleation

A given value of the Avrami exponent can be explained by various combinations of the nucleation mode, crystal growth geometry, and crystal growth rate. For example, an Avrami exponent of 3 can be interpreted either as athermally nucleated crystals with spherical symmetry and a linear growth rate or as thermally nucleated crystals with circular symmetry and a linear growth rate.[26] Therefore, for proper interpretation of the exponent, it is important to combine measurement of the Avrami exponent with observations of crystal growth geometry and growth rate.

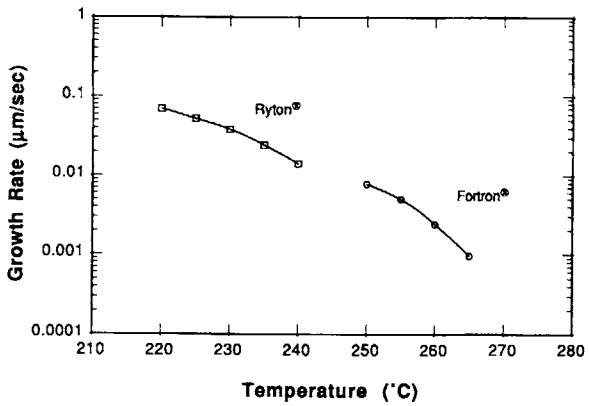

Figure 5 Spherulitic growth rates of Ryton® and Fortron® PPS.

As shown in Tables II and IV, the values of the Avrami exponent of unreinforced PPS were ~ 3. This information, when combined with the observations under the hot-stage microscope of equally sized, spherically symmetric spherulites, suggests that athermal nucleation is a good approximation to the mode of nucleation that occurs in this temperature range. For higher crystallization temperatures (265°C and above), nuclei were found to activate more sporadically in time. Therefore, at high temperatures, athermal nucleation cannot fully describe the nucleation process in PPS.

Evaluation of Bulk Nucleation Density

The bulk nucleation density of PPS was estimated from a relationship that exists between the Avrami rate constant, the spherulitic growth rate, and the bulk nucleation density. When the crystallization of an unreinforced polymer is governed by athermal nucleation of ideal three-dimensional spherulites with constant growth rates, the bulk nucleation density, N_b, can be estimated by

$$N_b = \left(\frac{3K'}{4\pi G^3}\right) \tag{2}$$

where K' is the Avrami rate constant for this idealized crystallization process. It should be recognized that in order for Eq. (2) to be dimensionally consistent, the units of K' must have dimensions $[\text{time}]^{-3}$, which corresponds to an Avrami exponent of exactly 3. Because the experimentally measured values of the Avrami exponent were slightly less than 3, the experimental values of K were adjusted

so that their units corresponded to those of ideal 3-D spherulites ($n = 3$). The following relationship, which adjusts the Avrami rate constant for a constant crystallization half-time, was used:

$$K' = \frac{(\ln 2)}{\left(\frac{\ln 2}{K}\right)^{3/n}} \quad (3)$$

In Eq. (3), K and n are the experimentally determined Avrami parameters, and K' is the adjusted Avrami rate constant with units that corresponded to a crystallization with $n = 3$. Avrami parameters obtained from DSC crystallizations of unreinforced PPS were combined with spherulitic growth rates from the microscopy experiments to calculate N_b as a function of crystallization temperature. It was assumed that the bulk nucleation density in the reinforced and unreinforced systems is the same because the specimens were subjected to the same thermal history. Qualitative observations of spherulites grown in the hot stage confirmed that the bulk nucleation density was approximately the same in the reinforced and unreinforced samples.

Tables VI and VII show the temperature dependence of the bulk nucleation densities of Ryton® and Fortron® in their corresponding crystallization windows. The bulk nucleation densities of both types of PPS increase slightly as the crystallization temperature decreases, an effect that has been observed before.[35] It is most striking, however, to compare the magnitudes of N_b for the two polymers. Ignoring the minor influence of crystallization temperature, the bulk nucleation density of Fortron® is more than 10^4 times greater than that of Ryton®. Usually, differences in N_b of this magnitude are due to the presence of nucleating agents; however, the PPS samples we studied were described as being free of additives. One possible explanation is that catalyst or reaction byproducts that serve as nucleating agents are incorporated into Fortron® during the polymerization process.

Whatever the cause of the higher bulk nucleation density of Fortron®, the difference in N_b for the two types of PPS is consistent with optical microscopy observations. For example, bulk nucleation densities

Table VI Bulk Nucleation Density of Ryton® PPS (Nuclei/cm³)

Polymer	225°C	230°C	235°C	240°C
Ryton®	7×10^7	4×10^7	3×10^7	3×10^7

Table VII Bulk Nucleation Density of Fortron® PPS (Nuclei/cm³)

Polymer	250°C	255°C	260°C	265°C
Fortron®	2×10^{12}	1×10^{12}	1×10^{12}	1×10^{12}

approximated from thin film specimens crystallized in the hot stage and the N_b values calculated using Eq. (2) agreed to within an order of magnitude. In addition, the estimated bulk nucleation densities of the two polymers are consistent with the extent to which reinforcing fibers influenced their crystallization kinetics (see Figs. 2 and 4). As demonstrated by computer simulation, the effect of fibers on the crystallization rate of polymers with relatively low bulk nucleation densities is greater than the effect of fibers on the crystallization rate of polymers with relatively high bulk nucleation densities.[24,29-31]

Evaluation of Fiber Nucleation Density

Fiber Nucleation Density of Ryton® PPS

Once the values of G, N_b, V_f, and D were determined as a function of temperature for the systems under consideration, a three-dimensional computer simulation[24,30] was used to estimate fiber nucleation densities. To estimate N_f for a given system at a given crystallization temperature, a number of simulations were run in which four of the controlling parameters were set to the experimentally measured values, while the fifth (N_f) was allowed to take on a range of values. Crystallization rate data from these simulation runs were then compared to the experimental crystallization rate data. The value for N_f was determined by the simulation data that "best fit" the experimental data in the range $0.03 < C < 0.60$. The data were not compared at higher values of the relative crystallinity because this is where delayed crystallization processes that are not considered in the simulation, such as secondary crystallization and annealing, become important. Comparisons between experimental and simulation data were made by "eyeball" fitting rather than by a more rigorous quantitative approach. This was considered to be reasonable in view of the errors inherent in the experimental data. It is important to emphasize that the value of N_f determined using the aforementioned method is based on the nominal surface area of the fiber, not the actual specific surface.

An example of the foregoing procedure used to evaluate N_f for a Ryton®/sized glass fiber system at a crystallization temperature of 225°C is shown in

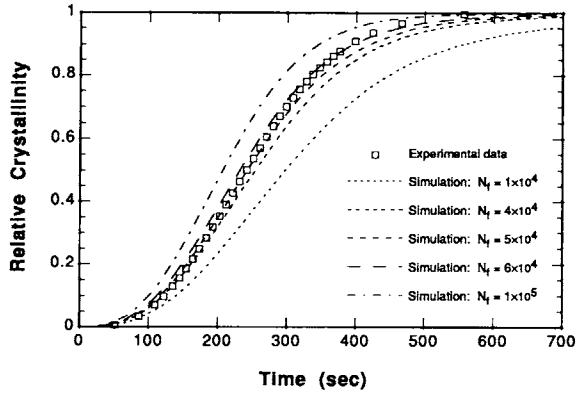

Figure 6 Comparison of experimental Ryton® PPS/sized glass crystallization data with simulation crystallization data at T_c = 225°C. Values of the controlling parameters are G = 0.052 μm/s, $N_b = 7.2 \times 10^7$ nuclei/cm^3, V_f = 0.45, D = 15 μm, and N_f (nuclei/cm^2) as indicated.

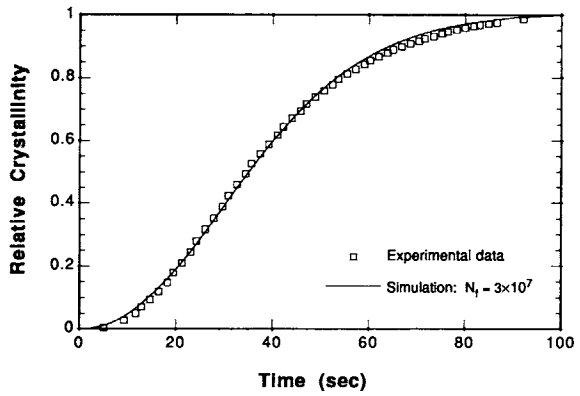

Figure 7 Comparison of experimental Ryton® PPS/Thornel® crystallization data with simulation crystallization data at T_c = 230°C. Values of the controlling parameters are G = 0.038 μm/s, $N_b = 4.2 \times 10^7$ nuclei/cm^3, $N_f = 3 \times 10^7$ nuclei/cm^2, V_f = 0.51, and D = 8 μm.

Figure 6. By examining the curves in Figure 6, a value for the fiber nucleation density that corresponds closely to the experimental data in this system is 5×10^4 nuclei/cm^2. A similar evaluation of a Ryton®/Thornel® composite at T_c = 230°C, shown in Figure 7, led to a fiber nucleation density of 3×10^7 nuclei/cm^2. For the Thornel® fiber-reinforced system, the simulation and experimental data coincide for nearly all values of C. Since secondary processes are not considered by the simulation, the close correspondence between experimental and simulation data even at high relative crystallinities suggests that secondary crystallization can be ignored for this system. In Figure 8, a comparison between experimental crystallization kinetic data for the four Ryton® fiber-reinforced systems and crystallization kinetic data generated with the simulation at T_c = 240°C is shown. The simulation curves represent the best fits to the experimental data that were achieved by varying only the fiber nucleation density. It is apparent that the simulation data agree well with the experimental data for all four fiber-reinforced systems at low values of C; however, the simulation significantly overpredicts the crystallization rate in the Ryton®/Kevlar® system at high relative crystallinities. The deviation between the experimental and simulation data may be the result of delayed crystallization processes that dominate at later times, but the deviation is significantly larger than that observed for other fiber types. Apparently, Kevlar® fibers affect the crystallization process of Ryton® in an unusual manner, as has been suggested by previous investigators.[6-8]

Fiber nucleation densities in the four fiber-reinforced Ryton® systems are summarized in Table VIII. It is interesting to note that within the accessible temperature window, the effect of crystallization temperature is small. One would expect that the fiber nucleation density would decrease with increasing crystallization temperature, but we were unable to obtain Ryton® crystallization data of high enough confidence outside of the range 225°C to 240°C to confirm this expected trend. In terms of the N_f values for the different fiber types, the ordering of the values in Table VIII is in agreement with the fiber effects observed in the Ryton® systems experimentally. Thornel® and Kevlar® fibers showed the largest enhancement of crystallization rate, and these fibers have the highest values of N_f. Glass and AS-4 carbon fibers were less effective at increasing the crystallization rate, and these fibers have rela-

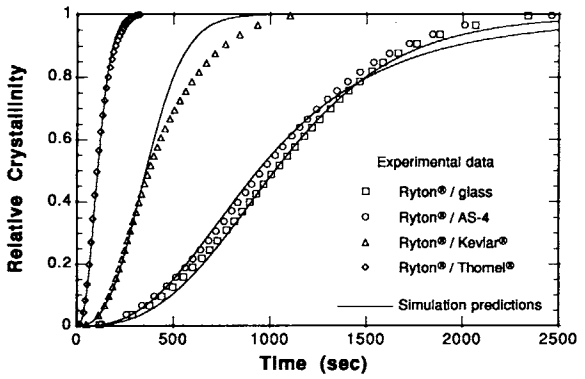

Figure 8 Comparison of experimental and simulation crystallization data for Ryton® PPS composites at T_c = 240°C. Values of the controlling parameters are G = 0.014 μm/s and $N_b = 3.1 \times 10^7$ nuclei/cm^3. Values for N_f, V_f, and D depend on the fiber type.

tively low values of N_f. Because the relative ordering of fiber effects on the crystallization rate of Ryton® so strongly correlates with the values of N_f, it is clear that the fiber nucleation density is the most influential fiber related parameter. Small variation in the fiber diameter and fiber volume fraction among the Ryton® composites had a relatively minor impact on the overall crystallization kinetics as compared to the fiber nucleation density.

Fiber Nucleation Density of Fortron® PPS

Attempts were made to carry out a similar quantitative analysis to evaluate the fiber nucleation densities in Fortron® composites. Because reinforcing fibers have such a small effect on the crystallization kinetics of Fortron® (see Figs. 3 and 4), it is not possible to use our method to estimate values of N_f with a reasonable level of accuracy. However, it is possible to demonstrate that fiber nucleation densities in the Fortron® systems were lower than some maximum value. Figure 9 shows a number of simulated crystallization curves for unreinforced and reinforced polymer with parameters that correspond to those of Fortron® composites. The figure demonstrates that changing N_f from 0 to 10^7 nuclei/cm^2 has a minimal effect on the crystallization kinetics of a polymer with a relatively high N_b. In fact, for a polymer with a bulk nucleation density of 2×10^{12} nuclei/cm^3, a fiber nucleation density of about 10^8 nuclei/cm^2 is necessary for a composite to crystallize marginally faster than the unreinforced polymer. Since no experimental reinforced Fortron® system crystallized more quickly than the base polymer, we can infer that the fiber nucleation densities of the aramid, carbon, and glass fibers in Fortron® PPS are less than 10^8 nuclei/cm^2.

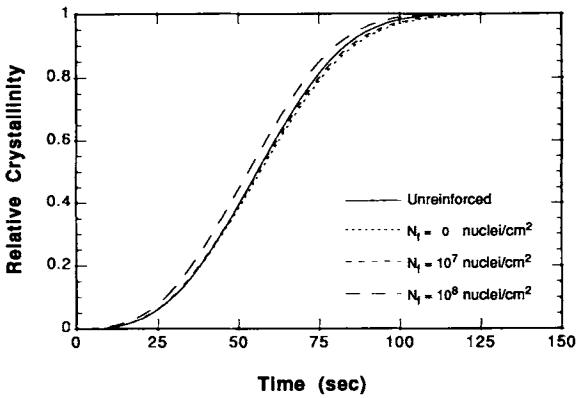

Figure 9 Effect of fiber nucleation density on crystallization rates for systems with $G = 0.0078$ μm/s, $N_b = 2 \times 10^{12}$ nuclei/cm^3, $V_f = 0.53$, $D = 8$ μm, and N_f as indicated. These parameters correspond to those of a Fortron® PPS/carbon fiber composite having 53 vol % fibers.

CONCLUSIONS

A comprehensive investigation of the crystallization kinetics of two types of PPS was undertaken using differential scanning calorimetry to quantify the effects of fibers on the crystallization process. For the case of Ryton® PPS, the presence of Thornel® and Kevlar® fibers dramatically enhanced the rate of crystallization of the base polymer, while AS-4 carbon and glass fibers also increased the crystallization rate of PPS, but to a lesser extent. Reinforcing fibers were also found to influence the Avrami parameters of Ryton® PPS. The Avrami rate constant, a measure of the crystallization rate, was higher for fiber-reinforced systems than for the base polymer. At all crystallization temperatures and for all fiber types, the Avrami exponent of the reinforced systems was lower than that of the unreinforced polymer by a statistically significant amount. The decrease in the Avrami exponent for the reinforced systems is presumably due to spherulitic growth being truncated by the constraining network of fibers.

Unlike the crystallization of Ryton® PPS, the crystallization of Fortron® PPS is only moderately affected by the presence of fibers. For all crystallization temperatures, fiber-reinforced systems crystallized at virtually the same rate, which was marginally slower than the rate of the unreinforced polymer. When the crystallization kinetics of Fortron® systems were analyzed with the Avrami equation, Avrami parameters calculated at a given

Table VIII Fiber Nucleation Densities of Ryton® PPS Composites (Nuclei/cm^2)

System	225°C	230°C	235°C	240°C
Ryton®/Thornel®	—	3×10^7	2×10^7	2×10^7
Ryton®/Kevlar®	2×10^6	2×10^6	1×10^6	1×10^6
Ryton®/AS-4	6×10^4	5×10^4	5×10^4	6×10^4
Ryton®/Glass	5×10^4	4×10^4	5×10^4	5×10^4

temperature for both unreinforced and reinforced systems were essentially indistinguishable.

From the results of this experimental study, it can be concluded that the crystallization of PPS depends on the characteristics of the fiber as well as the polymer. Reinforcing fibers that dramatically affect the crystallization of one type of PPS may have only a minor influence on the crystallization of another kind of PPS. This observation may explain why reports of fiber-induced effects on the crystallization of PPS are sometimes in disagreement.

A new method of quantifying the nucleation process that occurs in fiber-reinforced composites has been developed. The method, which is based on a comparison between experimental crystallization kinetic data and crystallization kinetic data predicted with a three-dimensional computer simulation, has been successfully applied to PPS composites reinforced with glass, carbon, and aramid fibers.

In analyzing the nucleation processes that occur in the PPS-based composites used in this study, it was determined that the bulk nucleation density of Fortron® PPS is more than 10^4 times higher than the bulk nucleation density of Ryton® PPS. This large difference in N_b was used to explain why the presence of reinforcing fibers has such a pronounced effect of the crystallization kinetics of Ryton® but has a negligible effect on the crystallization kinetics of Fortron®. The simulation was used to quantify the fiber nucleation densities in fiber-reinforced Ryton® composites, and the values of N_f were consistent with the relative fiber effects observed experimentally. An attempt was also made to quantify the fiber nucleation density in the Fortron® composites, but the high bulk nucleation density of the polymer prevented an estimation of N_f with any reasonable level of accuracy. It was possible, however, to predict that the crystallization rate of Fortron® would be relatively unaffected by varying the fiber nucleation density from 0 to 10^7 nuclei/cm^2. Thus, the value of N_f in reinforced Fortron® systems is not as important as it is in reinforced Ryton®.

Although the computer simulation was applied to polymer systems with a relatively simple crystallization mechanism (athermal nucleation and linear spherulitic growth), it is also possible to consider systems in which the crystallization is characterized by thermal nucleation and nonlinear spherulitic growth. In addition, with the measured values of N_f, it is possible to use the computer simulation to predict the crystallization kinetics and crystalline morphology of reinforced PPS for sets of parameters that were not studied experimentally. For example, the effect of changing fiber diameter and fiber volume fraction can easily be explored.

REFERENCES

1. J. L. Way, J. R. Atkinson, and J. Nutting, *J. Mater. Sci.*, **9**, 293 (1974).
2. G. Groeninckx, H. Berghmans, N. Overbergh, and G. Smets, *J. Polym. Sci. Polym. Phys. Ed.*, **12**, 303 (1974).
3. J. P. Jog and V. M. Nadkarni, *J. Appl. Polym. Sci.*, **30**, 997 (1985).
4. J. M. Kenny and A. Maffezzoli, *Polym. Eng. Sci.*, **31**, 607 (1991).
5. L. Caramaro, B. Chabert, J. Chauchard, and T. Vu-Khanh, *Polym. Eng. Sci.*, **31**, 1279 (1991).
6. G. P. Desio and L. Rebenfeld, *J. Appl. Polym. Sci.*, **39**, 825 (1990).
7. G. P. Desio and L. Rebenfeld, *J. Appl. Polym. Sci.*, **44**, 1989 (1992).
8. G. P. Desio and L. Rebenfeld, *J. Appl. Polym. Sci.*, **44**, 2005 (1992).
9. C. Auer, G. Kalinka, Th. Krause, and G. Hinrichsen, *J. Appl. Polym. Sci.*, **51**, 407 (1994).
10. H. Zeng and G. Ho, *Die Ange. Makromol. Chemie.*, **127**, 103 (1984).
11. Y. Lee and R. S. Porter, *Polym. Eng. Sci.*, **26**, 633 (1986).
12. C. N. Velisaris and J. C. Seferis, *Polym. Eng. Sci.*, **26**, 1574 (1986).
13. A. J. Waddon, M. J. Hill, A. Keller, and D. J. Blundell, *J. Mat. Sci.*, **22**, 1773 (1987).
14. L. C. Lopez and G. L. Wilkes, *ACS Polymer Preprints*, **30**, 207 (1989).
15. L. C. Lopez and G. L. Wilkes, *JMS—Rev. Macromol. Chem. Phys.*, **C29**, 83 (1989).
16. B. S. Hsiao and E. J. H. Chen, in *Proceedings of the Third International Conference on Composite Interfaces (ICCI-III)*, May 21–24, 1990, Cleveland, OH, H. Ishida, Ed., Elsevier Science Publishing Co., New York, 1990, p. 613.
17. B. S. Hsiao, I. Y. Chang, and B. B. Sauer, *Polymer*, **32**, 2799 (1991).
18. E. J. H. Chen and B. S. Hsiao, *Polym. Eng. Sci.*, **32**, 280 (1992).
19. V. E. Reinsch and L. Rebenfeld, *Polym. Comp.*, **13**, 353 (1992).
20. J. L. Thomason and A. A. van Rooyen, *J. Mater. Sci.*, **27**, 889 (1992).
21. J. L. Thomason and A. A. van Rooyen, *J. Mater. Sci.*, **27**, 897 (1992).
22. P. J. Phillips and A. J. Greso, *Proc. SPE ANTEC '92*, **27**, 779 (1992).
23. J. D. Menczel and G. L. Collins, *Polym. Eng. Sci.*, **32**, 1264 (1992).

24. N. A. Mehl, Ph.D. dissertation, Department of Chemical Engineering, Princeton University, 1994.
25. N. A. Mehl and L. Rebenfeld, *Polym. Eng. Sci.*, **32,** 1451 (1992).
26. B. Wunderlich, *Macromolecular Physics,* Vol. 2, *Crystal Nucleation, Growth, Annealing,* Academic Press, New York, 1976.
27. R. S. Stein and J. Powers, *J. Polym. Sci.*, **56,** S9 (1962).
28. N. Billon, J. M. Escleine, and J. M. Haudin, *Colloid Polym. Sci.*, **267,** 668 (1989).
29. N. A. Mehl and L. Rebenfeld, *J. Polym. Sci. Polym. Phys. Ed.*, **31,** 1677 (1993).
30. N. A. Mehl and L. Rebenfeld, *J. Polym. Sci. Polym. Phys. Ed.*, **31,** 1687 (1993).
31. N. A. Mehl and L. Rebenfeld, *ACS Proc. Polym. Mater. Sci. Eng.*, **67,** 96 (1992).
32. N. A. Mehl and L. Rebenfeld, *J. Polym. Sci. Polym. Phys. Ed.*, **33,** 1249 (1995).
33. M. Avella, G. Della Volpe, E. Martuscelli, and M. Raimo, *Polym. Eng. Sci.*, **32,** 376 (1992).
34. P. Cebe and S.-D. Hong, *Polymer,* **27,** 1183 (1986).
35. L. C. Lopez and G. L. Wilkes, *Polymer,* **29,** 106 (1988).
36. A. J. Lovinger, D. D. Davis, and F. J. Padden, Jr., *Polymer,* **26,** 1595 (1985).

Received September 9, 1994
Accepted January 10, 1995